



Regular article

Single-reference-based solution for two-point nonuniformity correction of infrared focal plane arrays

Songtao Chang*, Zhou Li

Changchun Institute of Optics, Fine Mechanics and Physics, Chinese Academy of Sciences, Changchun 130033, China

A B S T R A C T

Among numerous nonuniformity correction (NUC) algorithms, two-point calibration-based NUC is the most effective and commonly-used one for scientific and commercial infrared imagers. However, conventional two-point NUC requires two references at different level of flux, which is sometimes difficult to achieve in field applications. To overcome the restriction, a single-reference-based solution for two-point nonuniformity correction of infrared focal plane arrays is proposed in this paper. A single reference, which is easy to obtain, and a spherical reflecting warm shield are required to conduct this NUC method. The design method of this warm shield is developed. Several NUC experiments were performed to validate the proposed method. The experimental results indicate that the proposed NUC method yields almost equivalent performance with the conventional two-point NUC method, moreover it is economical and convenient in practical applications.

1. Introduction

Infrared imagers, also known as thermal imagers, have been used in military, scientific and commercial applications. A conventional infrared imager is composed of an infrared detector and an optical system, supported by other mechanical and electronic components. Infrared Focal Plane Arrays (IRFPAs) consisting of two dimensional detector arrays are the most popular infrared detectors nowadays. However, the IRFPAs suffer from undesired spatial nonuniformity owing to the nonuniform response of the individual detectors when illuminated by the same level of irradiance [1,2]. Despite significant advances in detector technology, the spatial nonuniformity remains a serious problem leading to degradation of images obtained with an infrared system. A number of papers and patents that address this problem have been published in recent years. NUC methods fall into three categories consisting of calibration-based techniques, scene-based techniques and shutter-less NUC [3]. Calibration-based NUC methods, such as single-point NUC, two-point NUC and multi-point NUC, have the benefit of providing radiometrically accurate imagery, although at the cost of periodically obstructing camera operation [4]. Scene-based techniques, which exploit only the information in the scenes being imaged avoids the disadvantages of the calibration-based techniques, whereas cause loss of radiometrical accuracy [5–7]. High-end and scientific infrared imagers are usually required to produce absolutely calibrated images in units of temperature or radiance, rather than just non-uniformity corrected images [8,9]. Hence scene-based NUC techniques are not applicable in such applications. Shutterless NUCs aim to remove dependence on blackbody or other uniform radiation sources

[10–16]. They are designed for convenience while loss as little performance as possible, compared with calibration-based NUCs. Refs. [10,11] present two real-time nonuniformity correction algorithms based on FPA temperature to compensate for nonuniformity caused by FPA temperature fluctuation. First, gain coefficients are calculated using a two-point correction technique. Then offset parameters at different FPA temperatures are obtained and stored in tables. When the camera operates, the offset tables are called to update the current offset parameters via a temperature-dependent interpolation. Essentially, these shutterless methods are designed to compensate offset non-uniformity caused by ambient or FPA temperature fluctuation. They are suitable for uncooled detectors rather than cooled detectors with constant FPA temperature. According to the literatures [17–20], the advantage of multi-point NUC is that it can solve some non-linear problems of detector response. For detectors with non-linear response, its correction performance is better than that of two-point NUC. However, the responses linearity of high performance infrared detectors are so excellent that multi-point NUC is almost not better than two-point NUC, on the contrary, multi-point NUC has some obvious disadvantages. It is known that multi-point NUC requires several uniform scenes at different temperatures. On the one hand, multiple uniform correction sources at different temperatures, or a blackbody source changing temperature by heating or cooling, are required to perform multi-point NUC. On the other hand, multi-point NUC increases the pressure of detector data processing, which is not acceptable to detectors working at high frame rate. Two-point calibration-based NUC, at present, is the most effective and commonly-used method for nonuniformity correction [3]. This type of technique can obtain more accurate correction

* Corresponding author.

E-mail address: stchang2010@sina.com (S. Chang).

results than single-point NUC. Whereas, many additional devices (e.g., blackbody sources, electromechanical parts, etc.) are required, therefore increases the size and the cost of infrared imaging systems. As a consequence, two-point NUC for infrared systems are usually performed at the factory or as a maintenance action, which is conducted once a month or longer. However, the spatial nonuniformity, including the gain and the offset, tends to drift slowly and randomly with time, so a one-time factory calibration will not provide a permanent solution to the problem [5]. This problem becomes even more challenging in uncooled infrared systems. In this case, it is required that the nonuniformity be corrected repeatedly during the course of camera operation. The current solution is a combination of two-point correction and single-point correction. Two-point correction is used as a default setting, and the single-point correction is conducted frequently to remove the effects mentioned above. Unfortunately, the single-point correction performs poor when the temperature of targets varies. Therefore it is not always applicable.

In this paper, a single-reference-based solution for two-point NUC is proposed to decrease the cost and complexity of conventional two-point NUC method. A short outline is presented as follows: in Section 2, the principles and shortcomings of single-point NUC and conventional two-point NUC are analyzed. In Section 3, the design method of the spherical reflecting warm shield, which can be used to change the incident flux, is proposed. Hence the single-reference-based two-point NUC method can be achieved with the help of a spherical reflecting warm shield. Several NUC experiments are performed to verify the theories described above in Section 4. It is concluded in Section 5 that the proposed method improves the convenience of two-point NUC while ensuring well performance.

2. Calibration-based NUC

Infrared systems, in many applications, are operated in a range of irradiance within which detectors exhibit linear input-output characteristics. The output gray value (DN, digital number) of a single detector is given by the approximate linear relation [21,22]:

$$Y_{i,j}^{(k)} = G_{i,j}^{(k)} \times X^{(k)} + O_{i,j}^{(k)} + \sigma_{i,j}^{(k)}, \quad (1)$$

where k denotes the frame number. $G_{i,j}$ and $O_{i,j}$ are respectively the gain and offset of the (i, j) th detector, and X denotes the true infrared radiance of the imaging target. $\sigma_{i,j}$ refers to the temporal noise which can be effectively reduced by averaging 20 or more frames. In general, gains and offsets of pixels are different, and NUC intends to draw them to uniform. After NUC, the calibration formula, Eq. (1), should be theoretically corrected to

$$\bar{Y} = \bar{G} \times X + \bar{O} \quad (2)$$

where \bar{Y} denotes the average of pixel outputs, \bar{G} is the corrected gain, and \bar{O} is the corrected offset. Actually, the desired response of each detector to the uniform radiation is the average of pixel outputs, namely \bar{Y} . The purpose of NUC is just to correct the response of each detector to the uniform radiation to be uniform. However, it does not mean that the gain and offset are corrected to the mean ones, that is to say Eq. (2) does not holds.

2.1. Single-point NUC

The principle of single-point NUC can be generally described by Fig. 1. It requires a single reference source, such as a blackbody radiator, a black-coated lens cap, a uniform sky area (without cloud and smoke), or other uniform scenes. The corrected responses of detectors are a' , b' , and c' , it can be seen that single-point NUC can only achieve the correction of offset $\beta_{i,j}$.

In order to remove the effect of temporal noise on NUC performance, 20 frames are acquired to calculating single-point NUC coefficients. Given the radiant temperature of the reference source or scene

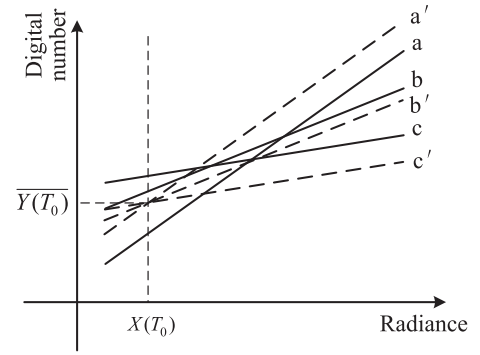


Fig. 1. Schematic diagram of single-point NUC.

T_0 , then the radiance of the scene can be expressed as $X(T_0)$. NUC of detectors can be executed by looking at the reference source, the average digital number of the obtained image can be denoted by

$$\bar{Y}(T_0) = \sum_{i=1}^M \sum_{j=1}^N Y_{i,j}(T_0), \quad (3)$$

where $M \times N$ is the number of individual detectors of an IRFPA. Correction coefficients of pixel (i, j) can be given by the following equation

$$\beta_{i,j}(T_0) = \bar{Y}(T_0) - Y_{i,j}(T_0) \quad (4)$$

As shown in Fig. 1, radiance of the reference source is $X(T_0)$, the response line of three pixels changed from a , b and c to a' , b' and c' after single-point correction. It is apparent that the correction performance is perfect at $X(T_0)$, whereas it degrades seriously when scene temperature changes. Suppose the temperature of an imaging scene is T , then the correction error of single-point NUC can be given by

$$\begin{aligned} \Delta Y_{i,j}(T) &= \bar{Y}(T) - [Y_{i,j}(T) + \beta_{i,j}(T_0)] \\ &= [\bar{Y}(T) - \bar{Y}(T_0)] - [Y_{i,j}(T) - Y_{i,j}(T_0)] \\ &= (\bar{G} - G_{i,j}) \cdot [X(T) - X(T_0)] \end{aligned} \quad (5)$$

Theoretically, the error of single-point NUC equals to 0 only in two cases. One is $T = T_0$, that is to say temperature of the reference source for NUC equals to that of the imaging scene. The other is $\bar{G} = G_{i,j}$, which means that gains of all pixels in an IRFPA are identical. However it is impossible for almost all IRFPAs. Eq. (5) demonstrates that the reality correction error is in direct proportion to $X(T) - X(T_0)$, meaning that greater temperature difference leads to worse performance of single-point NUC. For field applications, the lens cap or a uniform sky background can be used for single-point NUC, which performs quite well when imaging scenes or targets are at normal temperature (close to that of the reference source). However, there will be an evident degradation when imaging targets at higher or lower temperatures. Although it seems acceptable for applications of infrared target imaging and tracking, the drawbacks of single-point NUC is fatal for target identification and radiometry.

2.2. Two-point NUCS

The most widespread technique for nonuniformity correction is two-point NUC, which employs a blackbody radiator at different temperatures to correct both the gain and the offset. For a cooled or high-end infrared imaging system, the response of each pixel is linear to the incident radiance. Therefore two-point NUC provides satisfactory performance. Similar to the single-point NUC described above, 20 frames are required to remove the effect of temporal noise. To conduct two-point NUC, two reference resources, respectively at low temperature T_l and high temperature T_h , provided by a surface-area blackbody radiator, are essentially required. Suppose the blackbody temperature is

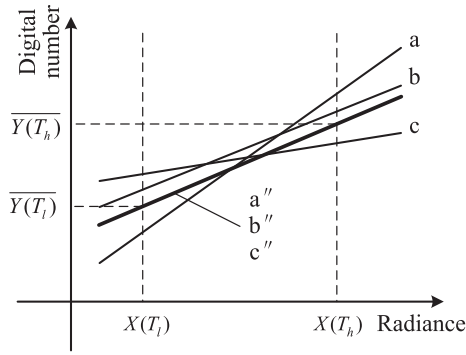


Fig. 2. Schematic diagram of two-point NUC.

set to a low temperature T_l and a high one T_h , respectively. According to the detector response formula Eq. (1), we obtain

$$\begin{cases} Y_{i,j}(T_l) = G_{i,j} \times X_{i,j}^{(k)}(T_l) + O_{i,j}^{(k)} \\ Y_{i,j}(T_h) = G_{i,j} \times X_{i,j}^{(k)}(T_h) + O_{i,j}^{(k)} \end{cases} \quad (6)$$

The basic principle of two-point NUC is shown in Fig. 2. a, b, and c are the response curves of the detector pixels before calibration. The corrected response curves a'', b'', and c'' are coincident, that is, the response of each pixel is the same.

Gain and offset correction coefficients of two-point NUC are respectively expressed as

$$\begin{cases} \alpha_{i,j} = \frac{\bar{Y}(T_h) - \bar{Y}(T_l)}{\bar{Y}_{i,j}(T_h) - \bar{Y}_{i,j}(T_l)} \\ \beta_{i,j} = \bar{Y}(T_h) - \alpha_{i,j} \bar{Y}_{i,j}(T_h) \end{cases} \quad (7)$$

Despite providing radiometrically accurate corrected imagery, two-point NUC requires a blackbody radiator as the reference, which is inconvenient in many applications. Moreover, commercial infrared systems are usually not equipped with blackbody for cost reasons. As a consequence, two-point NUC for infrared systems are usually performed at the factory or as a maintenance action, which is conducted once a month or longer. However, the performance of default two-point NUC coefficients can be degraded by changing of the ambient temperature, the optical system and the stray radiation. It is therefore necessary that NUC coefficients should be updated repeatedly, which poses a great challenge to the conventional two-point NUC method. To overcome this practical difficulty, we designed a spherical reflecting warm shield, and proposed a single-reference-based two-point NUC technique for infrared imaging systems.

3. Proposed NUC method

The f-number, defined as ratio of the system's focal length to the diameter of the entrance pupil, of an infrared imaging system can be changed by aperture stops or shields. Imaging a single uniform scene, the radiant energy received by infrared detectors is inversely proportional to square of the f-number as a rough estimate.

A single uniform scene is imaged by infrared detectors, as illustrated in Fig. 3. A_t and A_i are respectively the imaged target area and

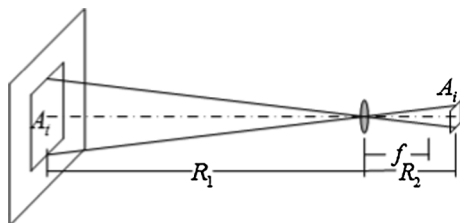


Fig. 3. Imaging of a uniform scene.

corresponding image area in FPA. R_1 and R_2 are the object distance and image distance, respectively.

Then the radiant flux received by a single pixel in the imaging area can be expressed by:

$$\begin{aligned} \Phi_{i,j}(T_i) &= \frac{\pi L(T_i) \cdot A_d \cdot \tau_{opt} \tau_{atm}}{4} \cdot \left(\frac{D}{f}\right)^2 \cdot \frac{R_1^2}{R_1^2 + (D/2)^2} \\ &= \frac{\pi L(T_i) \cdot A_d \cdot \tau_{opt} \tau_{atm}}{4} \cdot \frac{R_1^2}{R_1^2 + (D/2)^2} \cdot \left(\frac{1}{f\#}\right)^2, \end{aligned} \quad (8)$$

where $L(T_i)$ is radiance of the uniform scene at temperature T_i , A_d is the area of a single pixel, τ_{opt} and τ_{atm} are the transmittance of the detector and the atmosphere, $f\# = f/D$ is f-number of the infrared detector and the optical system. For a cooled infrared detector, f denotes the distance between the cold/warm shield and the detector, D is the clear aperture of the cold/warm shield. It can be seen that, for a given imaging system, the radiant energy received by a detector is inversely proportional to square of the f-number. It is worth noting that this relationship can be slightly affected by the optical system aberration and other factors. So the radiant energy received by infrared detectors is inversely proportional to square of the f-number as a rough estimate.

This is the essential principle of using warm shields, referring to uncooled optical shields in infrared technology, to achieve single-reference-based two-point NUC. Ordinary planar warm shields are not acceptable for infrared imaging systems because of introducing too much stray radiation. Although cold shields with adjustable clear aperture can achieve the change of f-number while introducing extraordinarily low stray radiation, the cost is not always acceptable for applications and the electromechanical systems are complicated. As a result, it is generally uneconomical to add cold shield only for the purpose nonuniformity correction. Fortunately, as a substitution, a specially designed spherical reflecting warm shield in this paper can achieve the change of f-number while introducing quite low stray radiation. It is naturally a good choice for single-reference-based two-point NUC.

3.1. Design of the spherical reflecting warm shield

The fundamental principle of the spherical warm shield design is to change the f-number of an infrared detector while introduction extraordinarily low irradiant flux. In general, the introduced radiation of a warm shield can be classified to two categories, namely the reflected flux and the emitted flux. In the other word, the detector cannot 'see' the ambient out of the field of view. According to the reversibility principle of ray path, all the rays traced from the infrared detector are completely reflected back to the cryogenic dewar by the designed spherical warm shield, as shown in Fig. 4. Additionally, the reflecting surface of the warm shield is polished and coated with high-reflection film, which has extraordinarily low emissivity compared with other objects. Principles of the spherical reflecting warm shield is demonstrated in Fig. 4, by appropriate design of surface curvature, position and outline dimension of the warm shield, ambient radiation outside the cold shield is unable to reach the detector directly or by reflecting. Moreover, emissivity of the spherical surface is extraordinarily low, so the amount of radiation introduced by the warm shield itself is extremely low.

As shown in Fig. 4, D_{ws} is dimension of the clear aperture, the distance between the clear aperture and the detector is denoted by S_{ws} . A Cartesian coordinate system is established with the detector center as the origin o . Axis ox points from the detector to the warm shield. Then the relationship between center of the spherical surface (x_c , 0) and radius of the reflecting surface R can be expressed as

$$R = \sqrt{(S_{ws} - x_c)^2 + D_{ws}^2/4}. \quad (9)$$

The cross section of the spherical reflecting surface is a portion of a circular arc, and the quadratic equation of the circle is given by

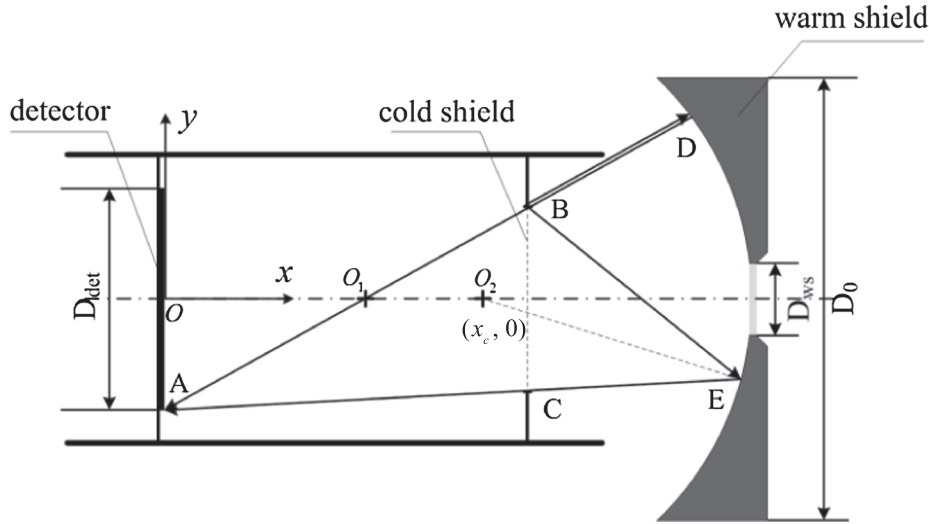


Fig. 4. Principle of spherical reflecting warm shield design.

$$[x - (S_{ws} - \sqrt{R^2 - D_{ws}^2/4})]^2 + y^2 = R^2. \quad (10)$$

Radius of the sphere is within a certain range to ensure that the external radiation cannot reach the detector by reflection of the warm shield. For simplicity, several critical rays are selected to determine the acceptable range of spherical radius. According to the principle of light reversibility, the external thermal background energy reaches the detector means that the detector can ‘see’ the background outside the cold shield. The IRFPA is in shape of rectangle, hence it obtain no incident flux as long as the rays emitted from four corners cannot reach the thermal environment background. The infrared optical system is rotational symmetric and the detector is axial symmetric, so that only one vertex A of the detector needs to be analyzed. D_{det} , in Fig. 4, is the diagonal length of the detector. According to the principle of spherical reflection and the analysis of geometric relations between the warm shield and the detector, it is found that if the ray in direction AB is reflected by point D to the edge point B, the radius of the reflecting spherical surface corresponds to maximum, namely R_{max} . The coordinate of point A and B are respectively $(0, -D_{det}/2)$ and $(S_{cs}, D_{cs}/2)$, where S_{cs} represents the distance between the cold shield and the detector, D_{cs} is the diameter of the cold shield. Thereupon the equation of line AB can be represented in the form of a straight line equation as

$$y = k_1 \cdot x + b_1, \quad (11)$$

where $k_1 = (D_{cs} + D_{det})/2S_{cs}$ and $b_1 = -D_{det}/2$.

According to the law of spherical reflection, the intersecting point of line AB and the axis ox is the center of sphere $(S_{cs} \cdot D_{det}/(D_{cs} + D_{det}), 0)$. Therefore the maximum radius of the spherical reflecting surface is

$$R_{max} = \sqrt{(S_{ws} - \frac{D_{det}}{D_{cs} + D_{det}} \cdot S_{cs})^2 + D_{ws}^2/4}. \quad (12)$$

Additionally, the critical ray AC originates from the positive edge of the detector diagonal line and passes through edge of the cold shield. It strikes at E on the reflecting surface, and after reflection it goes through edge of the cold shield. Infrared rays emitted by external thermal background travels along BECA path to the detector, whereby the path determines minimum radius R_{min} of the reflecting sphere. The coordinate of point C is, such that equation of line AC is given by

$$y = k_2 \cdot x + b_2. \quad (13)$$

where $k_2 = (-D_{cs} + D_{det})/2S_{cs}$ and $b_2 = -D_{det}/2$.

Submitting Eqs. (10)–(13) yields the coordinate of point E, expressed as $(x_E(R_{min}), y_E(R_{min}))$. Thereupon, the formula of line BE is given by

$$y = \frac{y_E(R_{min}) - D_{cs}/2}{x_E(R_{min}) - S_{cs}} \cdot (x - S_{cs}) + D_{cs}/2. \quad (14)$$

For simplicity, Eq. (14) can be written as

$$y = k_3 \cdot x + b_3, \quad (15)$$

where $k_3 = \frac{y_E(R_{min}) - D_{cs}/2}{x_E(R_{min}) - S_{cs}}$ and $b_3 = D_{cs}/2 - S_{cs} \cdot \frac{y_E(R_{min}) - D_{cs}/2}{x_E(R_{min}) - S_{cs}}$.

Assuming the coordinate of the sphere center is $O_2(x_c, 0)$, then line O_2E is the angular bisector of $\angle AEB$. According to the properties of angular bisector, the distance between point O_2 and line AC is equal to the distance between O_2 and line BE, such that

$$\frac{|k_2 \cdot x_c + b_2|}{\sqrt{k_2^2 + 1}} = \frac{|k_3 \cdot x_c + b_3|}{\sqrt{k_3^2 + 1}} \quad (16)$$

The coordinate of point E, namely $(x_E(R_{min}), y_E(R_{min}))$, can be determined by Eq. (13)–(16). Submitting $(x_E(R_{min}), y_E(R_{min}))$ to Eqs. (9) and (10), we can obtain R_{min} . It is computed by numerical solution in this paper.

The curvature radius of the warm shield is in the range of $R \in [R_{min}, R_{max}]$. In the other word, as long as radius of the reflecting surface falls into the range above, the detector can’t receive the infrared flux emitted by the external thermal background through the reflection of the spherical reflecting surface.

As shown in Fig. 4, $D(x_D, y_D)$ should be on the reflecting surface of a warm shield in order to prevent the external thermal background radiation from reaching the detector directly. The outline radius of a warm shield in oy axis must be larger than y_D , which can be obtained by solving Eqs. (10)–(11). Besides, diameter of the spherical reflecting surface limits the maximum outline diameter. In conclusion, outline diameter of the warm shield should be limited to $D_0 \in [2y_D, 2R]$.

3.2. Proposed NUC method using a warm shield

The single-reference-based two point NUC is realized by using a spherical reflecting warm shield. Fig. 4 shows the basic operation methods and principles. Instead of changing temperature of the correction reference, we change the incident flux that reaches the detector by inserting a specially designed warm shield to perform two-point NUC.

As shown in Fig. 5, clear aperture, referring to the central hole, of the warm shield is designed to ensure that the field angle determined by the cold shield is not influenced when it is installed at position P1. By imaging a uniform infrared reference, the first scene, which can be used as the high-temperature reference for two-point NUC, is obtained.

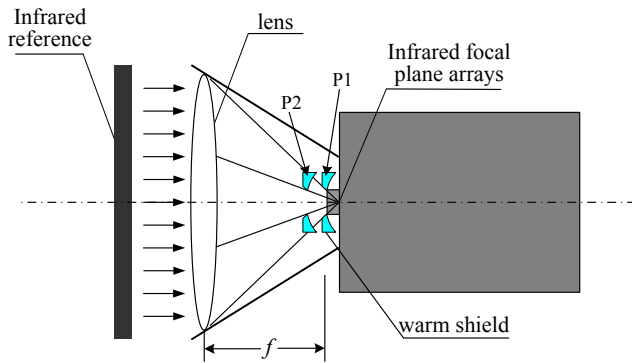


Fig. 5. Schematic illustration of single-scene-based two-point NUC.

When the warm shield is positioned at P2, f-number of the infrared imaging system and the incident radiation are both changed. It should be noted that, while the received energy of the IRFPA is reduced, all pixels or detectors are still uniformly irradiated. Thus the second reference is obtained by moving the warm shield to P2. It can be used as the low-temperature scene for two-point NUC. By this way, providing a single reference we can perform two-point NUC by using a spherical reflecting warm shield. The required single reference can be offered by a uniform lens cap, the sunny sky, a blackbody or other radiation sources. The proposed method, in principle, yields equivalent performance as conventional two-point NUC method based on blackbody, while it is superior to that of single-point NUC. Moreover, the correction reference is easy to obtain and the correction itself is easy to operate. So it is obviously superior to the conventional blackbody-based two-point NUC method in field environment practicality, convenience and cost.

4. Experimental results

4.1. Warm shield design and tests

To further evaluate the performance of the proposed single-reference-based two-point NUC method experimentally, a spherical reflecting warm shield is designed and fabricated. Meanwhile, an original planar warm shield is fabricated as well for comparison. Parameters of the warm shields were designed according an F2 cooled infrared system. Photo of the two warm shields is shown in Fig. 6. Following the theory in Section 3, a spherical reflecting warm shield is designed and the physical dimension is depicted in detail in Fig. 7 [23].

The reflecting surface of the warm shield is polished and coated with aluminum. According to the detection results, the average reflectivity is about 0.9 across the spectral band from $3.7\ \mu\text{m}$ to $4.8\ \mu\text{m}$, then the emissivity is therefore about 0.1. As a contrast, the planar warm shield is painted black with an emissivity of about 0.95. In order to measure stray radiation introduced by the two warm shields

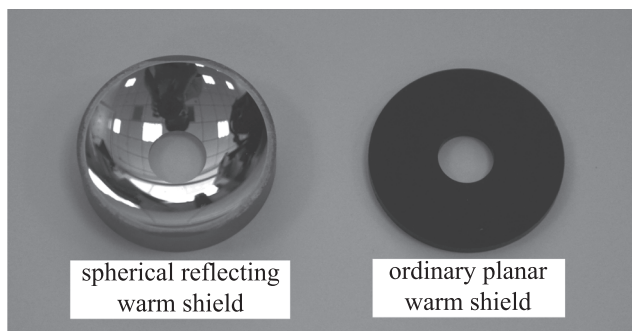


Fig. 6. Photo of warm shields.

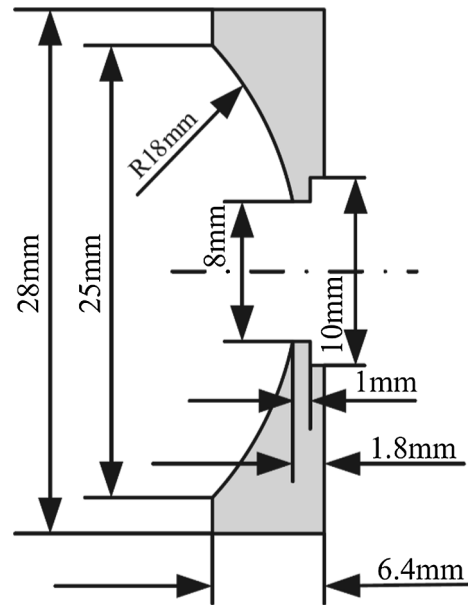


Fig. 7. Physical dimension of the spherical reflecting warm shield.

respectively, radiometric calibration experiments were performed with a MWIR camera having a large-scale MCT FPA (640×512 pixels). The extended area blackbody, selected as the reference source, has a 100×100 mm size and exhibits high effective emissivity (0.97 in $3.7\text{--}4.8\ \mu\text{m}$ waveband). As shown in Fig. 8, the experiments were conducted in a temperature test chamber. By changing the ambient temperature inside, stray radiation introduced by the two warm shields at different temperatures can be measured.

Three calibration experiments are conducted at each ambient temperature, one is calibration without warm shield, and the rest two are calibrations with a spherical reflecting warm shield and a planar one respectively. Subsequently, the stray radiation introduced can be obtained by subtracting the offset of the calibration equation with the warm shield and that of calibration without warm shield. According to the measurement results at different ambient temperatures indicated in Fig. 9, the stray radiation introduced by the spherical reflecting warm shield is about 9.5% of the ordinary planar one. Given the emissivity of the spherical reflecting warm shield is about 0.1, theoretical analysis shows that stray radiation introduced by it is about 10% of the ordinary planar warm shield. Considering temperature control error of the temperature test chamber, it shows that the spherical reflecting warm shield is well designed and the expected performance is achieved.

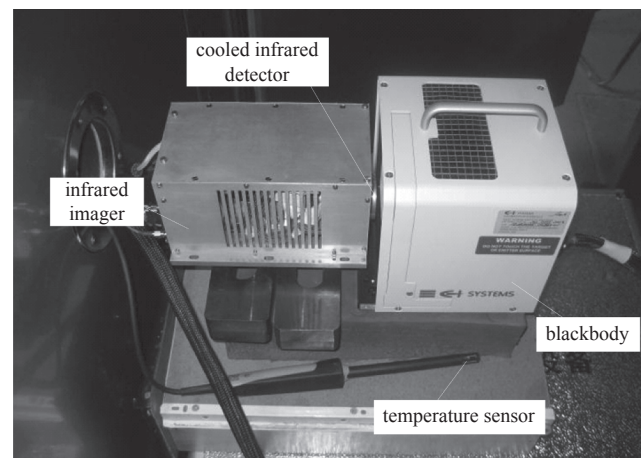


Fig. 8. Radiometric calibration in a temperature test chamber.

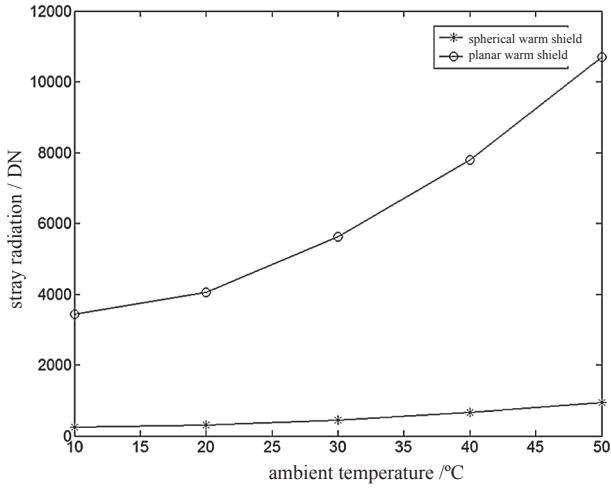


Fig. 9. Stray radiation introduced by two warm shields at different ambient temperatures.

4.2. Nonuniformity correction experiments

To verify the performance of the proposed NUC method in this paper, an MWIR camera is used for imaging and nonuniformity correction, as shown in Fig. 10. The extended area blackbody, selected as the reference source and the scene for imaging, has a 300 × 300 mm size and exhibits high effective emissivity (0.97 in 3.7–4.8 μm wave-band). Its temperature accuracy is about ± 0.02 °C over an operating temperature range of 0–150 °C. Besides, a lens cap with uniform black paint is used as another reference source to test the performance of the proposed NUC method.

To measure the performance qualitatively, three quality indexes are employed. The quality indexes are the national nonuniformity evaluation standard (NU), roughness index (ρ) and peak signal-to-noise ratio (PSNR) [24,25]. NU is the percentage of the root mean square deviation of effective pixel response with average response. It is defined as follows [26]:

$$\left\{ \begin{aligned} NU &= \frac{1}{\bar{DN}} \sqrt{\frac{1}{M \times N - d} \sum_{i=1}^M \sum_{j=1}^N (DN_{i,j} - \bar{DN})^2} \times 100\% \\ \bar{DN} &= \frac{1}{M \times N - d} \sum_{i=1}^M \sum_{j=1}^N DN_{i,j} \end{aligned} \right. \quad (17)$$

where \bar{DN} is the average digital number (DN) of pixels, d is the amount of defect pixels. The roughness index is used to measure the roughness in an image, which is defined as [27,28]:

$$\rho = \frac{\|h_1 * f\|_1 + \|h_2 * f\|_1}{\|f\|_1} \quad (18)$$

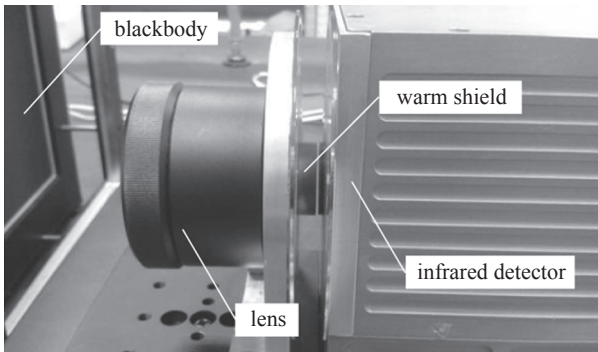


Fig. 10. Experimental setup for nonuniformity correction.

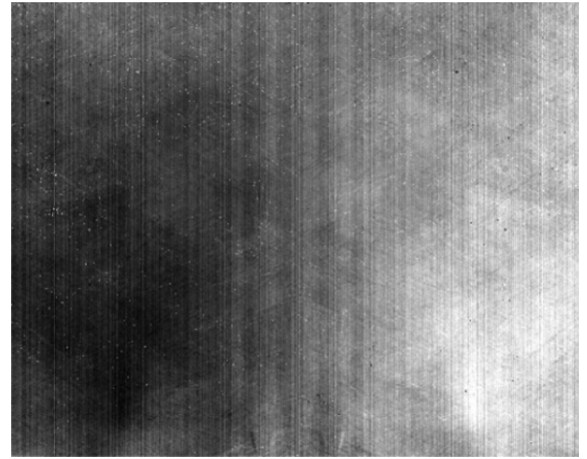


Fig. 11. Image of a scene at ambient temperature.

where h_1 is a horizontal mask [1, −1], $h_2 = h_1^T$ is a vertical mask, the asterisk denotes discrete convolution, and, for any image f , $\|f\|_1$ is its first-order norm. The PSNR is computed to show the difference between the reference image and an estimated image [29]:

$$PSNR = 10 \log_{10} \left(\frac{(2^{14})^2 \times MN}{\sum_{i=1}^M \sum_{j=1}^N (DN_{i,j} - \bar{DN})^2} \right) \quad (19)$$

NU and PSNR are suitable for evaluating the performance of NUC on uniform scenes, while ρ is quite effective for complex practical scenes [24–26].

The image of a uniform scene at ambient temperature is shown in Fig. 11. The scene is a blackbody working in the differential mode, and its temperature is 24.3 °C, which is equal to the ambient temperature. NU of the uncorrected image is 5.33%, which is unacceptable for infrared imaging. As can be seen, the image has obvious nonuniformity that characterized by stripes, dark spots, bright spots, and bright areas. It is therefore necessary to perform non-uniformity correction for the infrared imaging system.

To quantitatively evaluate the effectiveness of NUC methods, a uniform blackbody radiation source with variable temperatures was used as an imaging scene. The blackbody temperature is set to 20 °C, 25 °C, ..., 55 °C, and the NUC performances of scenes at these temperatures are evaluated. Two correction sources, namely a blackbody at ambient temperature and a uniform lens cap, are utilized to conduct the single-point NUC method respectively. Conventional two-point NUC method uses the blackbody at 20 °C and 30 °C as the high and low temperature reference respectively. The two temperature points are selected for the following reasons. (1) References at high temperatures are commonly provided by blackbodies, which are expensive and not available in some applications. Moreover, rising the temperature of a blackbody to higher is time consuming, and is not easy to operate. Therefore, it tends to select two low temperatures close to the ambient temperature, which are more convenient and practical. (2) This paper aims to propose an algorithm to achieve the two-point NUC with a single scene at ambient temperature, or low temperature. Therefore, two-point NUC performed at low temperatures, namely 20 °C and 30 °C, is more persuasive compared with that performed at higher temperatures.

For the proposed single-scene-based two-point NUC method, two calibration sources are used respectively. One is a blackbody at ambient temperature, it was used as the high temperature scene, and the low temperature scene is realized by inserting a spherical reflecting warm shield. The other reference is a lens cap, it was used as the high temperature scene, and the low temperature scene is realized by inserting a spherical reflecting warm shield. The blackbody at ambient

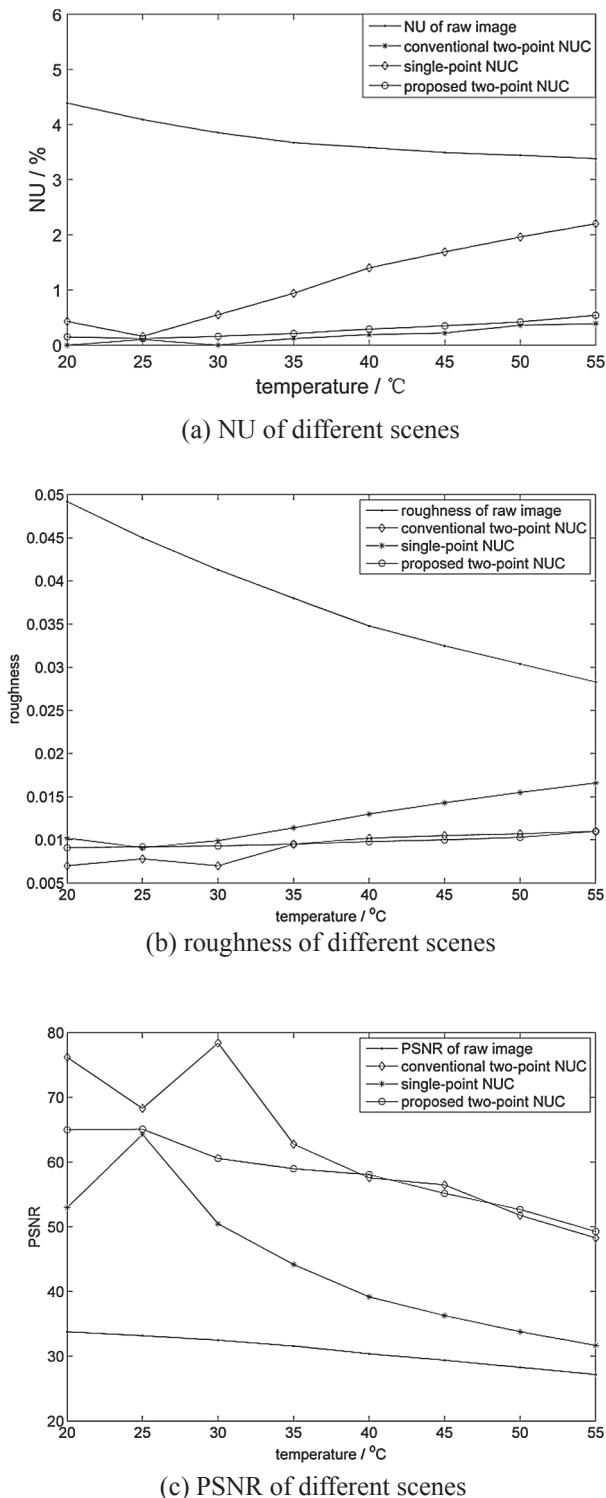


Fig. 12. Performance of blackbody-reference based NUC methods.

temperature, as a standard radiation source, was used to evaluate the optimal effect of the proposed NUC method. Whereas the lens cap, which can be replaced by other uniform scenes, is easy to implement in the field. In other words, it is the most convenient way to perform the proposed NUC method.

Blackbody-based single-point NUC and two-point NUC indicate the theoretical accuracy of the two nonuniformity correction methods. The

NU, roughness and PSNR of corrected images of scenes at different temperatures are shown in Fig. 12.

The scene to be corrected is provided by a uniform blackbody radiator with variable temperature. As shown in Fig. 12, the temperature of the scenes varies from 20 °C to 55 °C, 5 °C as the interval. These three figures illustrate that NU, roughness and PSNR performance of the proposed NUC method are equivalent to that of the conventional two-point NUC. We choose the national nonuniformity evaluation standard (NU), which is the most widely used one, to explain the performance of NUC methods in detail. The average NU of raw images without any correction techniques is 3.74%, which is unacceptable for infrared imaging or radiometry applications. Firstly, conventional two-point NUC method was adopted to correct the raw images. Blackbody at 30 °C and 20 °C are respectively used as the high and low temperature references. After correction, the average NUs of scenes at other different temperatures vary from 20 °C to 55 °C were decreased to 0.23%, which is about 6% of the raw images. The performance of two-point NUC is quite satisfactory.

Given that two-point NUC has the ability to correct gains and offsets of pixels perfectly in theory, the slightly increased NU is mainly resulted from the shot noise and the nonlinear response. The single-point NUC is performed with a blackbody at 24.3 °C, namely ambient temperature, as the single reference source. It can be seen that the performance of NUC is better when imaging scenes at temperatures that close to ambient temperature. For example, the residual NU of corrected images of scene at 25 °C is 0.16%, which is excellent for infrared imaging. When the scene temperature is far away from the ambient temperature, the performance of single-point NUC degrades rapidly. The NU of raw images at 55 °C, for instance, is 3.38% and decreased to 2.20% after single-point NUC, it is not acceptable for infrared imaging. The average gray level of a raw image at 55 °C is about 14000DN, which is close to the saturation of a 14 bit IRFPA. In this situation, the NU calculated here, for a corrected image at 55 °C, is almost equivalent to PRNU (Photo Response Non-uniformity) that defined by EMVA Standard 1288. Additionally, PRNUs of general industrial camera are recommended to be less than 1%. Therefore 2.20% here does not meet the requirements of infrared imaging.

In general, the experiments of single-point NUC are in agreement with the theoretical analysis in the previous sections. The proposed method, referring to single-reference-based two-point NUC, was carried out using a blackbody at ambient temperature (24.3 °C) as the single reference scene. The results in Fig. 12 demonstrate that the average NU of corrected images is 0.28%, which is almost equivalent to the conventional two-point calibration method. In conclusion, the single-point NUC is not a satisfactory nonuniformity correction method for the scene or target where the temperature is different from that of the correction reference. Conventional two-point NUC yields high precision and stability, and has strong adaptability to scenes or targets at different temperatures. The performance of the method proposed in this paper is almost equivalent to conventional two-point NUC.

Furthermore, the blackbody radiation source as a reference source for NUC will bring about an increase in cost and an inconvenient operation. For some low-cost infrared systems, it is not economical to equip a blackbody, which is quite expensive, only for nonuniformity correction. Working environments of military infrared systems are complicated, thereupon NUC is sometimes required to be conducted frequently to remove the effect of ambient temperature and internal heating. As a result, blackbody-based NUC may be not so practicable. Fortunately, almost all optical systems are equipped with a lens cap, which can be used as a substitute for blackbody. In this paper, black-coated lens cap is used as a uniform reference for single-point NUC and the proposed two-point NUC methods, the results are shown in Fig. 13.

The performance of single-point NUC using lens cap is similar to that of blackbody-based single-point NUC. With lens cap as a reference

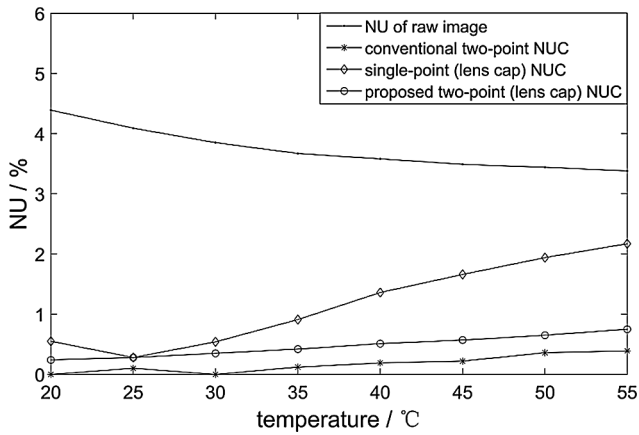


Fig. 13. Performance of NUC methods using a lens cap.

to implement the proposed NUC method in this paper, the average residual NU of scenes at 20 to 55 °C is 0.47%. The performance is worse than that of the blackbody-reference based method mentioned above owing to nonuniformity of lens cap, which is not so good as a blackbody. However, The residual NU is still acceptable for infrared imaging, and is significantly better than the single-point NUC. It is worthy noting that the correction performance does not deteriorate significantly when scene temperature changes. So lens cap is acceptable for conducting the proposed two-point NUC method.

To further verify the proposed method in this paper, nonuniformity corrections were carried out for the image of a scene with targets at various temperatures. As shown in Fig. 14, the dark areas are targets at temperatures approximate to ambient temperature, and the brighter square area is a uniform radiator at about 50 °C. The raw image captured has obvious stripes and bright or dark spots, therefore the imaging is poor and required to be corrected.

Firstly, an ordinary planar warm shield was inserted between the lens and the detector to conduct the proposed NUC method. The corrected image is shown in Fig. 15(a), it looks a bit better than the raw image, but not acceptable for infrared imaging. It is proved that an ordinary warm shield is not suitable for the proposed NUC method. The image after single-point NUC is shown in Fig. 15(b), it is obvious that the performance of single-point NUC is favourable for the background area (at ambient temperature). However, there are some black spots in the bright area (target at 50 °C). The performance of single-point NUC therefore is not good enough for infrared imaging.

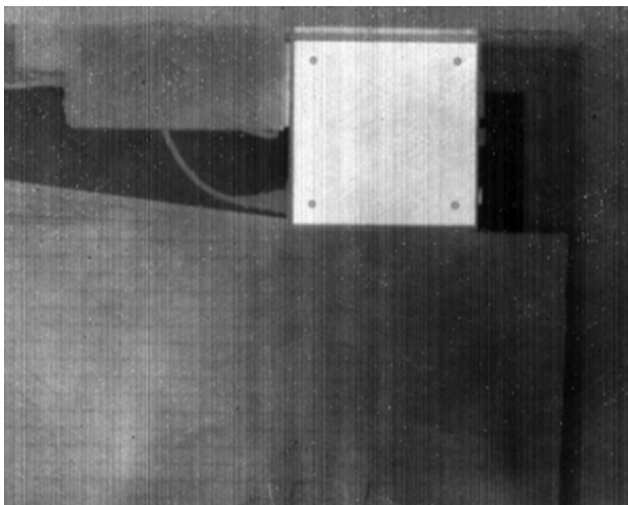
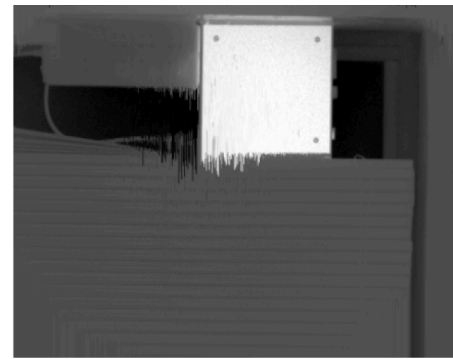
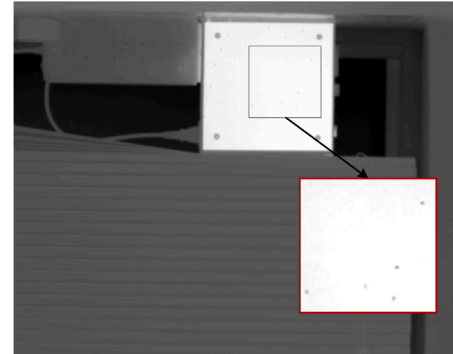


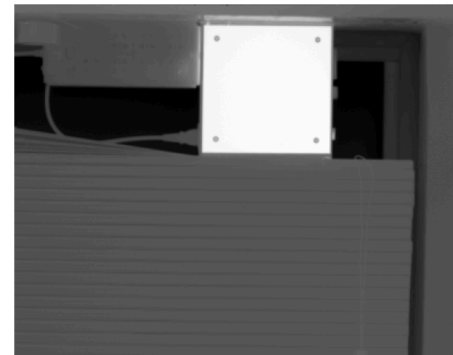
Fig. 14. Raw image of a practical scene (roughness index $\rho = 0.047$).



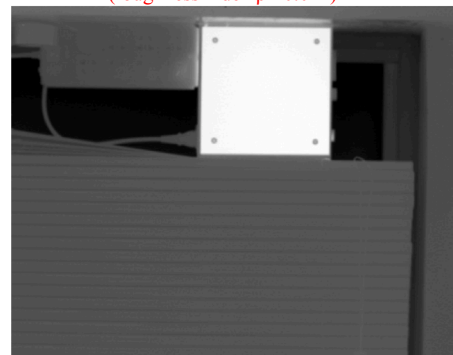
(a) proposed NUC method using a planar warm shield (roughness index $\rho = 0.035$)



(b) single-point NUC (roughness index $\rho = 0.023$)



(c) conventional two-point NUC (roughness index $\rho = 0.014$)



(d) proposed NUC method using a spherical reflecting warm shield (roughness index $\rho = 0.015$)

Fig. 15. Corrected images of a practical scene.

The performance of conventional two-point NUC is shown in Fig. 14(c). The correction results of both the high temperature and low temperature targets are satisfactory, and there are no obvious spots or stripes. As shown in Fig. 14(d), the proposed method can remove the

stripes and spots of the raw image effectively, and the correction performances of high and low temperature targets are almost equivalent to Fig. 14(c). In a word, the proposed method can effectively realize nonuniformity correction for targets at different temperatures, and the performance is comparable with that of conventional two-point NUC.

Based on analysis of the correction performance of uniform scenes as well as an actual imaging scene, the proposed method has excellent adaptability and the performance is close to that of conventional two-point correction. In general, It is an economical and convenient two-point correction scheme, which is suitable for various commercial and military infrared imaging systems. It is worth noting that the correction is always calculated for power lower than the power that will be explored during the mission. However, this drawbacks is negligible for infrared detectors with linear response, while it is obvious for infrared detectors with poor performance. The conventional and the proposed two-point NUC methods are not applicable for detectors with poor performance, i.e. bad linearity. Besides, we suggest that the non-uniformity correction of cooled infrared system should be carried out again in a few hours under stable environment. If the uniformity requirement is high or the working environment is poor, the NUC should be conducted more frequently.

5. Conclusion

This paper introduces a single-reference-based two-point NUC method based on a spherical reflecting warm shield. It achieves two-point NUC with only one common target or scene such as lens cover and sky background. Firstly the essential principle and drawbacks of conventional single-point NUC and two-point NUC are introduced. Then, the design method of a spherical warm shield is proposed, it acts as the key element to achieve single-reference-based two-point NUC. The design method of the spherical reflecting warm shield is proposed. Experimental results indicate that the stray radiation introduced is extremely low, hence it can be used for NUC. Correction results of uniform references, namely a blackbody and a lens cap, show that the proposed two-point NUC yields almost equivalent performance with conventional two-point NUC, and is far better than single-point NUC. In addition, a practical image of a complicated scene was corrected by several NUC methods, and the proposed NUC method was proved to be effective. It is worth noting that performance of the proposed two-point NUC will degrade if the temperatures of some objects in the scene are too high, for example higher than 55 °C. The reference source, at ambient temperature, for NUC shall be replaced by a uniform scene at higher temperature to solve this problem.

The main advantages of the approach developed in this paper are listed as bellow: (1) it yields almost the same performance comparing to conventional two-point NUC; (2) it does not require expensive references, such as the blackbody, thus saving the cost and benefitting the operator; (3) it improves the efficiency of NUC, as well as gives the user the freedom to update the NUC coefficients timely.

Declaration of Competing Interest

The authors declared that there is no conflict of interest.

Appendix A. Supplementary material

Supplementary data to this article can be found online at <https://doi.org/10.1016/j.infrared.2019.06.007>.

References

- [1] D. Zhou, D. Wang, L. Huo, R. Liu, P. Jia, Scene-based nonuniformity correction for airborne point target detection systems, *Opt. Express* 25 (12) (2017) 14210–14226.
- [2] B. Gutschwager, J. Hollandt, Nonuniformity correction of imaging systems with a spatially nonhomogeneous radiation source, *Appl. Opt.* 54 (36) (2015) 10599–10605.
- [3] F. Marcotte, P. Tremblay, V. Farley, Infrared camera NUC calibration: comparison of advanced methods, *Proc. SPIE* 8706 (2014) 870603.
- [4] Y. Jin, J. Jiang, G. Zhang, Three-step nonuniformity correction for a highly dynamic intensified charge-coupled device star sensor, *Opt. Commun.* 285 (2012) 1753–1758.
- [5] Y. Cao, C. Tisse, Single-image-based solution for optics temperature-dependent nonuniformity correction in an uncooled long-wave infrared camera, *Opt. Lett.* 39 (3) (2014) 646–648.
- [6] Z. He, Y. Cao, Y. Dong, J. Yang, Y. Cao, C. Tisse, Single-image-based nonuniformity correction of uncooled long-wave infrared detectors: a deep learning approach, *Appl. Opt.* 57 (2018) D155–D164.
- [7] S.N. Torres, J.E. Pezoa, M.M. Hayat, Scene-based nonuniformity correction for focal plane arrays using the method of the inverse covariance form, *Appl. Opt.* 42 (2003) 5872–5881.
- [8] M. Ochs, A. Schulz, H.-J. Bauer, High dynamic range infrared thermography by pixelwise radiometric self calibration, *Infrared Phys. Technol.* 53 (2010) 112–119.
- [9] T. Svensson, I. Renhorn, Evaluation of a method to radiometric calibrate hot target image data by using simple reference sources close to ambient temperature, *Proc. SPIE* 7662 (2010) 76620X.
- [10] X. Huang, X. Sui, Y. Zhao, An efficient shutter-less non-uniformity correction method for infrared focal plane arrays, *Proc. SPIE* 10250 (2016) 102500K.
- [11] Y. Cao, C. Tisse, Shutterless solution for simultaneous focal plane array temperature estimation and nonuniformity correction in uncooled long-wave infrared camera, *Appl. Opt.* 52 (2013) 884–889.
- [12] B. Cairnduff, Correction of non-uniformity of response in sensor arrays, G.B. patent 2 445 254 A, 7 October 2008.
- [13] Z. Jiang, Method for obtaining image correction coefficient of nonuniform images, involves calculating correction coefficient based on quadratic sum of average value difference of two groups of pixelvalues after correcting pre-corrected images, Chinese patent CN 102176742 A, 7 September 2011.
- [14] L. Huang, X. Sun, Non-uniformity correction method involves counting correlation coefficient according to current working temperature detector corresponding to current real time, Chinese patent CN 102768071, 7 November 2012.
- [15] P.W. Nugent, J.A. Shaw, N.J. Pust, Correcting for focal-plane array temperature dependence in microbolometer infrared cameras lacking thermal stabilization, *Opt. Eng.* 52 (2013) 061304.
- [16] Y. Cao, C.L. Tisse, Shutterless solution for simultaneous focal plane array temperature estimation and nonuniformity correction in uncooled long-wave infrared camera, *Appl. Opt.* 52 (2013) 6266–6271.
- [17] W. Isoz, T. Svensson, I. Renhorn, Nonuniformity correction of infrared focal plane arrays, *Proc. SPIE* 5783 (2005).
- [18] F. Marcotte, P. Tremblay, V. Farley, Infrared camera NUC and calibration: comparison of advanced methods, *Proc. SPIE* 8706 (2013).
- [19] M. Schultz, L. Caldwell, Nonuniformity correction and correctability of infrared focal plane arrays, *Infrared Phys. Technol.* 36 (1995) 763–777.
- [20] A. Friedenberg, I. Goldblatt, Nonuniformity two-point linear correction errors in infrared focal plane arrays, *Opt. Eng.* 37 (1998) 1251.
- [21] W.L. Wolfe, Introduction to Radiometry, SPIE, 1998.
- [22] G.C. Holst, Testing and Evaluation of Infrared Imaging Systems (JCD, 1933).
- [23] Q.J. Tian, S.T. Zhang, F.Y. He, Z. Li, Y.F. Qiao, Spherical warm shield design for infrared imaging systems, *Infrared Phys. Technol.* 85 (2017) 66–73.
- [24] K. Liang, C. Yang, L. Peng, B. Zhou, Nonuniformity correction based on focal plane array temperature in uncooled long-wave infrared cameras without a shutter, *Appl. Opt.* 56 (2017) 6266–6271.
- [25] M. Schulz, L. Caldwell, Nonuniformity correction and correctability of infrared focal plane arrays, *Infrared Phys. Technol.* 36 (1995) 763–777.
- [26] X. Sui, Q. Chen, G. Gu, A novel non-uniformity evaluation metric of infrared imaging system, *Infrared Phys. Technol.* 60 (2013) 155–160.
- [27] M.M. Hayat, S.N. Torres, E. Armstrong, S.C. Cain, B. Yasuda, Statistical algorithm for nonuniformity correction in focal-plane arrays, *Appl. Opt.* 38 (8) (1999) 772–780.
- [28] R. Lai, Y.T. Yang, Q. Li, X.L. Zhou, Improvement in adaptive nonuniformity correction method with nonlinear model for infrared focal plane arrays, *Opt. Commun.* 282 (2009) 3444–3447.
- [29] Y. Cao, M. Yang, C.L. Tisse, Effective strip noise removal for low-textured infrared images based on 1D guided filtering, *IEEE Trans. Circuits Syst. Video Technol.* 26 (2016) 2176–2188.